RESEARCH PAPER

The Akt inhibitor, triciribine, ameliorates chronic hypoxia-induced vascular pruning and TGFβ-induced pulmonary fibrosis

Maha Abdalla[1,2], Harika Sabbineni[1], Roshini Prakash[1], Adviye Ergul[1,3], Susan C Fagan[1,4] and Payaningal R Somanath[1,5,6,7]

[1]Clinical and Experimental Therapeutics, College of Pharmacy, University of Georgia and Charlie Norwood VA Medical Center, Augusta, GA, USA, [2]Department of Pharmaceutical Sciences, South College School of Pharmacy, Knoxville, TN, USA, [3]Department of Physiology, [4]Department of Neurology, [5]Department of Medicine, [6]Vascular Biology Center, and [7]Cancer Center, Georgia Regents University, Augusta, GA, USA

BACKGROUND AND PURPOSE

Interstitial lung disease accounts for a group of chronic and progressive disorders associated with severe pulmonary vascular remodelling, peripheral vascular rarefaction and fibrosis, thus limiting lung function. We have previously shown that Akt is necessary for myofibroblast differentiation, a critical event in organ fibrosis. However, the contributory role of the Akt-mTOR pathway in interstitial lung disease and the therapeutic benefits of targeting Akt and mTOR remain unclear.

EXPERIMENTAL APPROACH

We investigated the role of the Akt-mTOR pathway and its downstream molecular mechanisms in chronic hypoxia- and TGFβ-induced pulmonary vascular pruning and fibrosis in mice. We also determined the therapeutic benefits of the Akt inhibitor triciribine and the mTOR inhibitor rapamycin for the treatment of pulmonary fibrosis in mice.

KEY RESULTS

Akt$1^{-/-}$ mice were protected from chronic hypoxia-induced peripheral vascular pruning. In contrast, hyperactivation of Akt1 induced focal fibrosis similar to TGFβ-induced fibrosis. Pharmacological inhibition of Akt, but not the Akt substrate mTOR, inhibited hypoxia- and TGFβ-induced pulmonary vascular rarefaction and fibrosis. Mechanistically, we found that Akt1 modulates pulmonary remodelling via regulation of thrombospondin1 (TSP1) expression. Hypoxic Akt$1^{-/-}$ mice lungs expressed less TSP1. Moreover, $TSP1^{-/-}$ mice were resistant to adMyrAkt1-induced pulmonary fibrosis.

CONCLUSIONS AND IMPLICATIONS

Our study identified Akt1 as a novel target for the treatment of interstitial lung disease and provides preclinical data on the potential benefits of the Akt inhibitor triciribine for the treatment of interstitial lung disease.

Abbreviations

ECM, extracellular matrix; FHLF, fibrotic human lung fibroblast; FN, fibronectin; ILD, interstitial lung disease; IPF, idiopathic pulmonary fibrosis; mTOR, mammalian target of rapamycin; PH, pulmonary hypertension; PTEN, phosphatase and tensin homologue; SRF, serum response factor; TCBN, triciribine; TSP1, thrombospondin1; αSMA, α-smooth muscle cell actin

Table of Links

TARGETS
Enzymes
Akt1
mTOR
PI3 kinase

LIGANDS	
Bosentan	Pirfenidone
Everolimus	Rapamycin (sirolimus)
LY294002	SU5416 (semaxanib)
Nintedanib	Triciribine (Akt inhibitor V)

These Tables list key protein targets and ligands in this article which are hyperlinked to corresponding entries in http://www.guidetopharmacology.org, the common portal for data from the IUPHAR/BPS Guide to PHARMACOLOGY (Pawson *et al.*, 2014) and are permanently archived in the Concise Guide to PHARMACOLOGY 2013/14 (Alexander *et al.*, 2013).

Introduction

Interstitial lung disease (ILD) is characterized by reduced lung volume due, in part, to progressive hypertrophic scar formation leading to fibrosis and vascular remodelling (McLaughlin *et al.*, 2009; King *et al.*, 2011; Raghu *et al.*, 2011; Hinz *et al.*, 2012; Meyer, 2014). Although its pathogenesis is multifactorial, persistent myofibroblast accumulation and excess deposition of extracellular matrix (ECM) proteins are critical events in this fibro-proliferative process. Thus, identifying novel pathways is important in the hopes of devising new targeted therapeutics for pulmonary remodelling.

Research from our laboratory has established the central role of Akt1, a serine-threonine protein kinase Bα, in ECM assembly and secretion (Somanath *et al.*, 2007; Somanath and Byzova, 2009; Goc *et al.*, 2011). We previously reported that genetic ablation of Akt1 in mice resulted in impaired secretion and assembly of ECM proteins and enhanced angiogenesis leading to vascular leakage and skin abnormalities (Chen *et al.*, 2005a). Genetic knock-down of Akt1, not Akt2, resulted in impaired angiogenesis in cutaneous wound healing (Somanath *et al.*, 2008). We also demonstrated that sustained hyperactivation of Akt1 resulted in increased myofibroblast differentiation via increased α-smooth muscle cell actin (αSMA) synthesis involving serum response transcription factor (SRF) and myocardin (Abdalla *et al.*, 2013). Furthermore, pharmacological inhibition of Akt or genetic ablation of Akt1 impaired myofibroblast differentiation and ED-A fibronectin (ED-A-FN) synthesis *in vitro* (Abdalla *et al.*, 2013).

Myofibroblasts are the hallmark of pulmonary fibrosis (Raghu *et al.*, 2011; Hinz *et al.*, 2012). Pulmonary vascular remodelling in pulmonary hypertension (PH) has also been demonstrated to be mediated by adventitial myofibroblasts (Barman *et al.*, 2014). Our previous findings on the role of Akt-mTOR pathway in extracellular remodelling and myofibroblast differentiation suggest that Akt and/or mTOR may be potential targets for therapeutic interventions in ILD.

Other studies have also reported a possible correlation between Akt hyperactivation and fibrotic diseases. Mice deficient in the protein PTEN (phosphatase and tensin homologue), an endogenous inhibitor of Akt pathway, developed a fibroproliferative response consistent with fibrosis (Xia *et al.*, 2010). Interestingly, Akt expression has been found to be elevated in fibrotic lung tissues from patients with idiopathic pulmonary fibrosis (IPF) (Xia *et al.*, 2008). However, the precise role of the Akt-mTOR pathway in the pathogenesis of pulmonary fibrosis and the therapeutic benefits of targeting Akt and mTOR in ILD remain unknown.

In this study, we investigated the contributory role of Akt in general, and Akt1 in particular, in pulmonary tissue remodelling. We identified that $Akt1^{-/-}$ mice are protected from hypoxia-induced pulmonary fibrosis and vascular remodelling and that adenovirus-mediated overexpression of hyperactive Akt1 (adMyrAkt1) in mouse lungs resulted in increased fibrosis. Pharmacological inhibition of Akt using triciribine (TCBN) significantly reversed TGFβ- and chronic hypoxia-induced pulmonary fibrosis. However, targeting mTOR using rapamycin did not yield therapeutic benefits on chronic hypoxia- or TGFβ-induced pulmonary vascular rarefaction and fibrosis. Mechanistically, we found that genetic ablation of Akt1 and pharmacological inhibition of Akt were associated with impaired thrombospondin1 (TSP1) expression by the fibroblasts *in vitro* and in the lung tissues *in vivo*. Furthermore, $TSP1^{-/-}$ mice were protected from adMyrAkt1-induced fibrosis. Collectively, we identified Akt1 as a novel target in ILD as it is a critical mediator of hypoxia- and TGFβ-induced pulmonary remodelling, in part through TSP1 regulation.

Methods

Antibodies

Anti-αSMA, anti-TSP1 and anti-fibronectin antibodies were purchased from Sigma (St Louis, MO, USA). GAPDH,

phosphoAkt-S473, phosphoT37/46-4E-BP1 and anti-SRF antibodies were purchased from Cell Signaling (Boston, MA, USA). Anti-myocardin antibodies were purchased from R&D Systems (Minneapolis, MN, USA). Collagens type I and III antibodies were purchased from Rockland (Gilbertsville, PA, USA). Antibodies for ED-A-FN, collagen VI and αSMA were purchased from Abcam (Cambridge, MA, USA).

Cell culture

Normal and fibrotic human lung fibroblasts (FHLFs) and FGM™-2 fibroblast growth medium-2 were purchased from Lonza (Walkersville, MD, USA). Normal human lung fibroblasts were cultured on a 6-well plate. After reaching 70% of confluence, cells were subjected to serum starvation in the presence or absence of 100 pM TGFβ (R&D Systems) for 48 h (Goc *et al.*, 2011). This was followed by co-treatment for 24 h (total 72 h) with inhibitors of PI3 kinase (25 μM LY294002), Akt (10 nM TCBN; 1,5-dihydro-5-methyl-1-β-D-ribofuranosyl-1,2,5,6,8-pentaazaacenaphthylen-3-amine) or mTOR (25 nM rapamycin), all of which are obtained from Calbiochem (Millipore, Billerica, MA, USA). Cells were subjected to Western analyses as described below. For FHLFs, cells were cultured in serum starvation in a 6-well plate and treated with inhibitors of Akt (10 nM TCBN) or mTOR (25 nM rapamycin) for 24 h.

Western blot analysis

Cell lysates were prepared using lysis buffer [20 mM Tris-HCl, pH 7.4; 1% Triton X-100, 3 mM EGTA, 5 mM EDTA, phosphatase inhibitors (10 mM sodium pyrophosphate, 5 mM sodium orthovanadate, 5 mM sodium fluoride and 10 μM okadaic acid), protease inhibitor cocktail (Roche Diagnostics, Basel, Switzerland) and 1 mM PMSF]. SDS-PAGE and Western blotting were performed as described previously (Abdalla *et al.*, 2013).

Animals

All animal care and experimental procedures were approved by the Charlie Norwood VAMC Institutional Animal Care and Use Committee. All studies involving animals are reported in accordance with the ARRIVE guidelines for reporting experiments involving animals (Kilkenny *et al.*, 2010; McGrath *et al.*, 2010). A total of 230 animals were used in the experiments described here.

Akt1$^{-/-}$ mice were generated as previously described (Chen *et al.*, 2005b) and were maintained in the C57BL/6 background. Age-matched male Akt1$^{+/+}$ and Akt1$^{-/-}$ (8–12 weeks old) mice were utilized for the chronic hypoxia and TGFβ-induced pulmonary fibrosis models. Eight-week-old male TSP1$^{-/-}$ mice were purchased from Jackson mice (Bar Harbor, ME, USA).

Chronic hypoxia model

Akt1$^{+/+}$ and Akt1$^{-/-}$ mice were subjected to normoxia or hypoxia (10% O$_2$) (Biospherix, New York, NY, USA) for 7 and 14 days (n = 2–6 mice per group). Noteworthy, high mortality was observed in Akt1$^{-/-}$ mice exposed to hypoxia longer than 14–16 days. For pharmacological inhibition studies, Akt1$^{+/+}$ mice, subjected to normoxia or chronic hypoxia for 14 days, received daily i.p. injection of saline, TCBN (0.5 mg·kg^{-1}·day^{-1}) or rapamycin (1.5 mg·kg^{-1}·day^{-1}) for 7

days, and the total continuous exposure to hypoxia or normoxia was 21 days (n = 6–8 mice per group). Pharmacological inhibitors were administered daily while the mice were maintained in the hypoxia chamber to minimize exposure to air and spontaneous reversal of pulmonary remodelling. After lung isolation, the left lung was subjected to histology for haematoxylin and eosin (H&E), Masson's trichrome and immunofluorescence staining against αSMA (to elucidate vascular remodelling) and fibronectin (to elucidate vascular and peripheral fibrosis). The right lung was subjected to Western analyses against various proteins including TGFβ, αSMA, myocardin, SRF, fibronectin, specialized fibronectin (ED-A), collagen (I, III, VI), phosphorylated Akt, mTOR, 4EBP, TSP1 and GAPDH.

Adenovirus administration

Mice were treated with intratracheal (i.t.) control adenovirus (adControl) or adenovirus TGFβ (adTGFβ) at a concentration of 1×10^6 pfu. Saline, TCBN or rapamycin was administered i.p. on days 7–10 (n = 6–8 mice per group). For the Akt-induced fibrosis experiment, TSP1$^{+/+}$ and TSP1$^{-/-}$ mice were subjected to i.t. administration of control vector or adenovirus expressing constitutively active-Akt1 (adMyrAkt1) two times on days 0 and 7. Mice were killed and lungs were collected on day 14.

Vascular Microfil® casting

Following completion of adenovirus or hypoxia studies, mice were anesthetized and given 50 μL of heparin (50 mg·mL^{-1}) subcutaneously. Microfil (FlowTech, Inc., Carver, MA, USA) casting agent (1:2 dilution + 3.2% curing agent) was infused through the right ventricle at a perfusion rate of 1 mL·min^{-1}. After curing for approximately 30 min, lungs were isolated, fixed in 4% paraformaldehyde overnight, and cleared with ethanol and methyl salicylate per the manufacturer's manual. After approximately 2 months of vascular clearing, the peripheral vasculature was imaged using confocal microscopy (n = 5–8 mice per group).

Histological and immunohistochemical assessments

Left lung lobe, heart and liver tissues were fixed in 4% paraformaldehyde, embedded in paraffin and sectioned at 5 μm thickness. Quantitative and qualitative evaluation of fibrotic changes was obtained as follows: Using ImageJ software (National Institutes of Health, Bethesda, MD, USA), the threshold percentage area for each field was averaged and presented as percentage of fibrosed area (3–6 fields per lung section per mouse). The severity of pulmonary fibrosis was scored (0–8 scale; 0 for normal and 8 for total fibrosis) in lung sections stained for collagen with Masson's trichrome stains using the grading system described previously (Ashcroft *et al.*, 1988). Immunostaining for αSMA and fibronectin was performed using specific antibodies. For vascular remodelling studies, lung sections from each animal were stained with H&E and Masson's trichrome and examined by digital photomicroscopy at various magnifications to determine the severity of the disease. Peripheral pulmonary vessels were examined to determine the medial wall/lumen diameter ratio, and the right ventricular wall thickness was measured

in heart sections (average of 8–10 measurements per animal per group) to determine right ventricular hypertrophy. Finally, liver morphology was assessed semi-quantitatively using the threshold in ImageJ software in 5 fields per liver section per mouse per group. All quantitative vascular remodelling assessments following Microfil casting were performed on binary images.

Quantitative RT-PCR arrays

Control pBabe (retroviral) and DN-Akt1 (Akt1 K179M) expressing NIH-3T3 fibroblasts and FHLFs were used for the qRT-PCR arrays. Briefly, cells were lysed and RNA was isolated using RNAase Mini plus Kit (Qiagen, Valencia, CA, USA) according to the manufacturer's instructions. Next, cDNA was generated by RT2 First Strand Kit (SABiosciences, Valencia, CA, USA), mixed with qPCR Sybr Green master mix and loaded into fibrosis RT2 Profiler PCR Array plates (SA Biosciences). Reading was completed in Eppendorf Mastercycler realplex-2 equipment (Hamburg, Germany).

Data analysis

Data are presented as means ± SD. Statistical analysis was performed using two-way ANOVA on the ranks of the data that were used to compare control, insult (chronic hypoxia or adTGFβ or adMyrAkt1), and control or insult, plus TCBN or rapamycin. Student's t-tests with a two-tailed distribution were used to compare control and treated as well as $Akt1^{+/+}$ and $Akt1^{-/-}$ mice on all variables. Statistical significance was determined at $P < 0.05$.

Results

Akt1$^{-/-}$ mice are resistant to chronic hypoxia-induced pulmonary remodelling

To examine whether Akt is required for pulmonary remodelling, $Akt1^{+/+}$ and $Akt1^{-/-}$ mice were subjected to normoxia, short-term hypoxia (7 days) or chronic hypoxia (14 days), and morphological alteration due to hypoxia was assessed. The results showed that $Akt1^{+/+}$ mice subjected to chronic hypoxia developed patterns consistent with the disease progression as evidenced by patchy lesions, mild vessel luminal narrowing and medial thickening on day 7 that progressed to diffuse interstitial lesions and significant vascular remodelling on day 14 (Figure 1A and B). In contrast, hypoxic $Akt1^{-/-}$ mice showed histopathological patterns similar to normoxic $Akt1^{+/+}$ mice on days 7 and 14 (Figure 1A and B). Despite chronic hypoxia exposure, $Akt1^{-/-}$ mice had minimal fibronectin accumulation in the interstitial space (Figure 1C and E). Furthermore, 14d-hypoxic $Akt1^{-/-}$ mice had normal appearing pulmonary arterioles as evidenced by the absence of any medial thickening and luminal narrowing, decreased αSMA assembly and decreased fibronectin deposition compared with $Akt1^{+/+}$ mice lungs (Figure 1D and F). Thus, results suggest that absence of Akt1 impedes hypoxia-induced pulmonary remodelling.

Interestingly, normoxic $Akt1^{-/-}$ mice exhibited morphological features similar to 14d-hypoxic $Akt1^{+/+}$ mice on tissue remodelling (Figure 1A–C) and vascular wall thickening as

well as αSMA expression (Figure 1D–F). Compared with normoxic $Akt1^{+/+}$ mice, genetic ablation of Akt1 was associated with increased interstitial thickening, αSMA and fibronectin deposition.

Akt inhibition reverses chronic hypoxia-induced pulmonary remodelling in vivo

Hypoxic vasoconstriction and vascular remodelling are one of the contributing factors in the pathogenesis of pulmonary fibrosis (Strange and Highland, 2005). In our study, severe chronic hypoxia (21 days) induced medial thickness of peripheral pulmonary arterioles, which correlated with increased collagens, fibronectin and αSMA deposition as demonstrated by H&E, Masson's trichrome and immunofluorescence staining respectively (Figure 2A). This was also confirmed at the protein level where hypoxia increased the levels of αSMA and its transcription factors, SRF and myocardin, and various ECM proteins (Figure 2C). TCBN treatment, administered for 7 days after 14 days of hypoxia until 21 days of hypoxia is reached, reversed the vascular thickening as shown by immunohistochemistry and Western analyses (Figure 2A–C). On the other hand, rapamycin treatment did not prevent hypoxia-induced pulmonary alveolar haemorrhage and congestion (Figure 2A–C). Noteworthy, under normoxic conditions, rapamycin alone induced mild tissue and vascular remodelling in the lungs (Figure 2A).

Akt inhibition reverses adTGFβ-induced pulmonary fibrosis in vivo

Next, we sought to investigate the effects of Akt inhibition using TCBN and mTOR inhibition using rapamycin on TGFβ-induced model of pulmonary remodelling. Administration of adTGFβ (i.t.) to mouse lungs induced significant damage in the normal pulmonary architecture that correlated with an Ashcroft fibrosis score of ~7.6 (categorized as severe fibrosis). Administration of adTGFβ resulted in a heterogeneous pattern consistent with advanced stage IPF (Figure 3A) with substantial interstitial fibrosis, ECM deposition, loss of alveolar parenchyma, microscopic honeycomb foci and an increase in the percentage of fibrosed area. This was also associated with marked increase in fibronectin and αSMA deposition and assembly as demonstrated by immunofluorescence staining (Figure 3A). Akt inhibition using TCBN blunted adTGFβ-induced fibrosis correlating to an Ashcroft fibrosis score of ~1.2 (categorized as minimal fibrosis) (Figure 3A–C). This is evidenced by markedly decreased fibrotic patches, ECM deposition and αSMA expression (Figure 3A–C). In contrast, although rapamycin-treated animals had decreased fibrotic patches and improved Ashcroft fibrosis score of ~5 (categorized as moderate fibrosis) (Figure 3A–C), they also demonstrated thickening of the alveolar space, diffuse alveolar micro-haemorrhage, capillary congestion and dense inflammatory infiltrates as evidenced by H&E and Masson's trichrome staining (Figure 3A). Notably, even in the absence of adTGFβ, control mice treated with rapamycin exhibited aberrant pulmonary morphological features (Figure 3A–C).
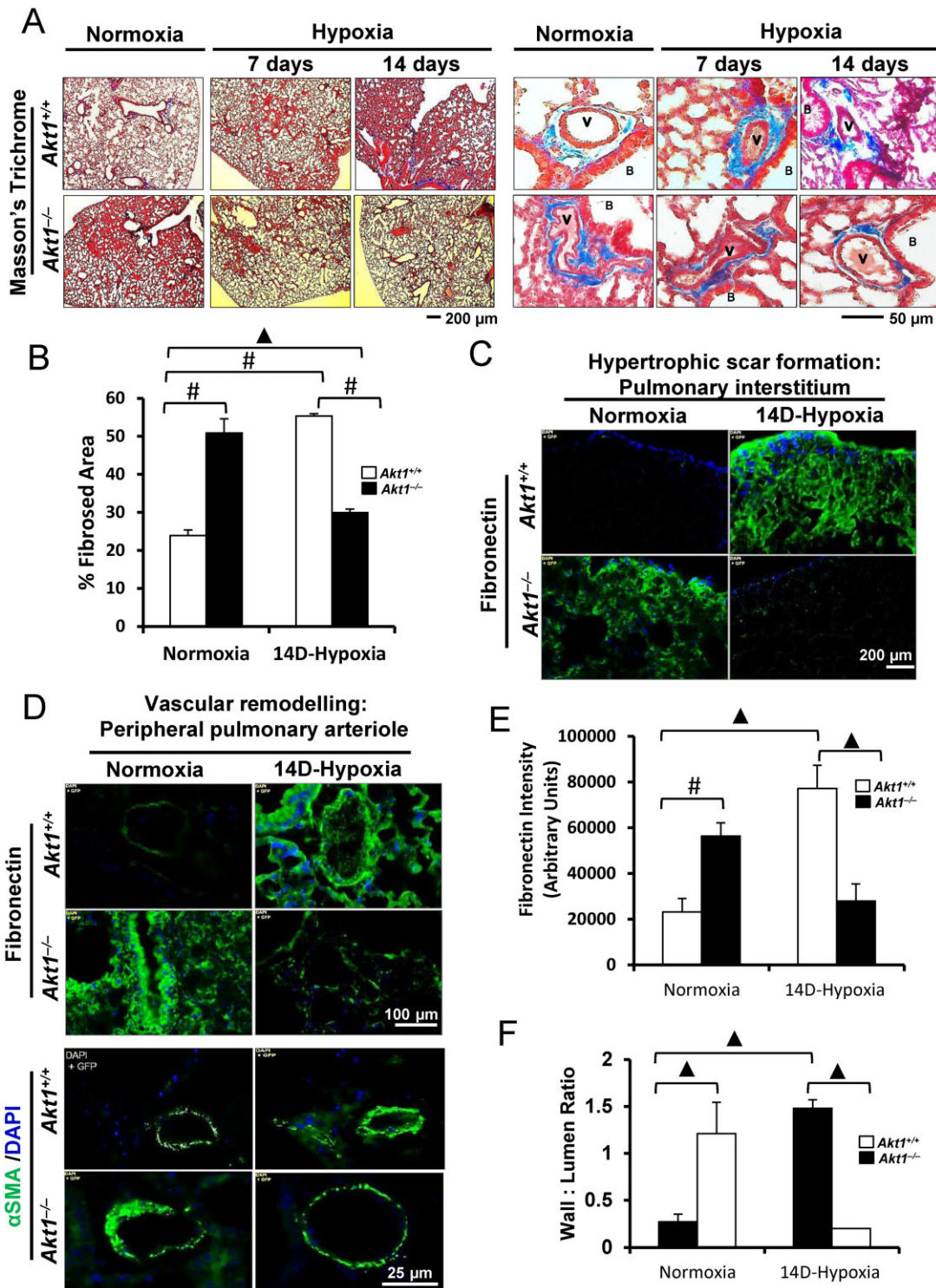
Figure 1

Akt1 deficiency protects against hypoxia-induced pulmonary remodelling. (A) Masson's trichrome stained section of the pulmonary interstitium (left) and peripheral pulmonary arterioles (right) of $Akt1^{+/+}$ and $Akt1^{-/-}$ mice subjected to normoxia or chronic hypoxia for 7 and 14 days ($n = 3–5$ mice/group). (B) Histogram showing quantification of the fibrosed area in $Akt1^{+/+}$ and $Akt1^{-/-}$ mice lungs after 14 day hypoxia compared with normoxia. (C) Immunostaining of frozen sections of 14 day hypoxia and normoxia $Akt1^{+/+}$ and $Akt1^{-/-}$ mice lungs showing fibronectin expression in the interstitium. (D) Fibronectin and αSMA immunofluorescence staining in and around small pulmonary arteries of normoxic and 14d-hypoxic $Akt1^{+/+}$ and $Akt1^{-/-}$ mice. (E) Histogram showing reduced fibronectin expression in $Akt1^{-/-}$ mice hypoxic lung sections compared with $Akt1^{+/+}$ mice lungs ($n = 4–5$ mice/group). (F) Histogram showing vascular wall to lumen ratio in $Akt1^{+/+}$ and $Akt1^{-/-}$ mice lung hypoxic sections measured from αSMA immunofluorescence ($n = 3–5$ mice/group). V, vasculature; B, bronchiole. $^{\#}P < 0.01$, $^{▲}P < 0.001$.
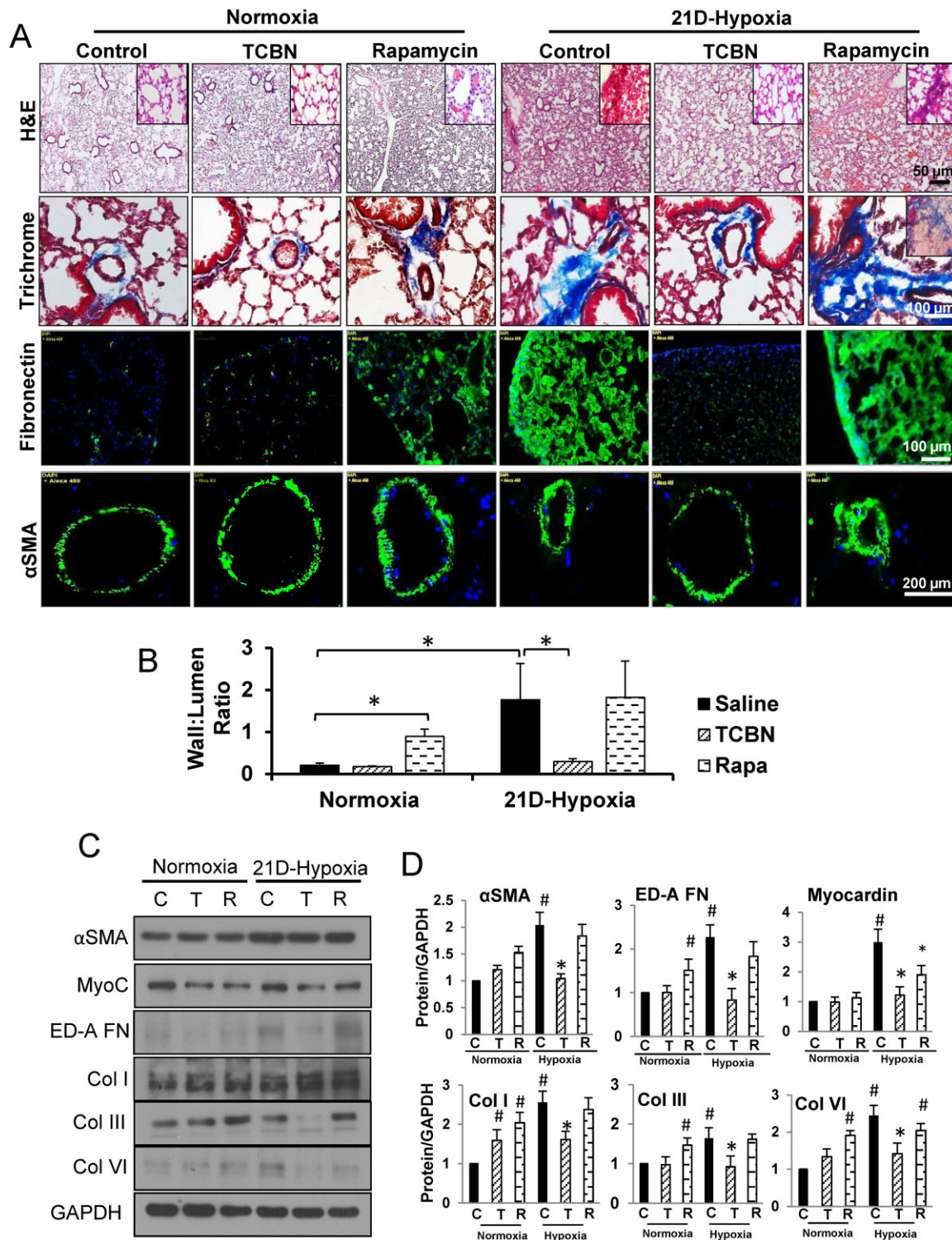
Figure 2

TCBN reverses hypoxia-induced pulmonary fibrosis and vascular remodelling *in vivo*. (A) H&E staining, Masson's trichrome staining, fibronectin and αSMA immunofluorescence staining of lung sections subjected for normoxia and 21 day chronic hypoxia. (B) Histogram showing vascular wall to lumen ratio ($n = 6$–8 mice/group). (C) Western analysis of αSMA and its transcription factors SRF and myocardin, ECM proteins including ED-A-FN, collagen types I, III and VI in TCBN, and rapamycin-treated lungs compared with vehicle-treated lungs after 21 days of hypoxia. (D) Histograms showing the densitometry analysis of Western protein bands showing changes in the expression of αSMA, SRF, myocardin, ED-A-FN, collagen types I, III and VI in control, TCBN and rapamycin-treated 21 day hypoxic lungs. $*P < 0.05$, $^\#P < 0.01$ ($n = 6$–8 mice/group).
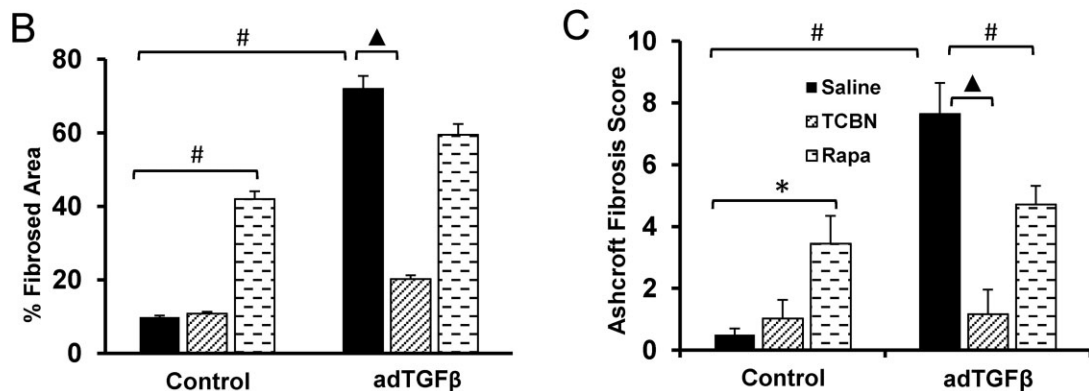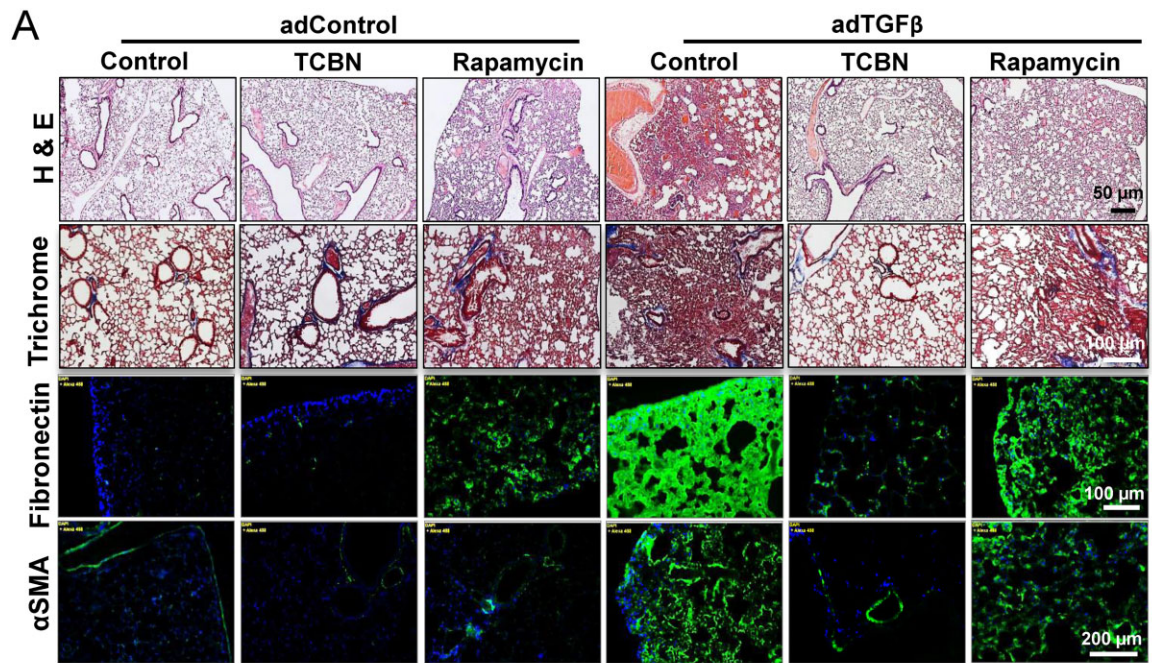
Figure 3

TCBN ameliorates adTGFβ-induced pulmonary fibrosis *in vivo*. (A) H&E staining, Masson's trichrome staining, fibronectin and αSMA immuno-fluorescence staining of lung sections subjected for adControl and adTGFβ treatments. (B) Histogram showing quantification of the fibrosed area in adControl and adTGFβ-expressing mice lungs (n = 6–8 mice/group). (C) Histogram showing Aschroft fibrosis score in adControl and adTGFβ-expressing mice lungs (n = 6–8 mice/group). *P < 0.05, #P < 0.01, ▲P < 0.001.

Akt inhibition ameliorates hypoxia- and adTGFβ-induced peripheral vascular rarefaction

The above findings prompted us to examine the effects of Akt inhibition on the aberrant peripheral vascular rarefaction that occurs during PH and pulmonary fibrosis (PF). To do this, we utilized arterial casting to visualize the vascular tree of mouse lungs subjected to 21d-chronic hypoxia and/or adTGFβ. First, compared with the diffuse vascular blush observed in the normoxic lung, chronic hypoxia resulted in significant vascular pruning as demonstrated by binary images of peripheral vessels (Figure 4A and B). TCBN partially inhibited progressive pruning of the vasculature (Figure 4A and B), which supports our previous finding that TCBN alle-

viates vessel occlusion in microcapillaries. In contrast, rapamycin treatment did not significantly reverse the reduced vascular density due to chronic hypoxia and had no significant effect on pruning of small vessels (Figure 4A and B). Noteworthy, while TCBN did not modulate vascular density in normoxic mice, rapamycin was associated with vascular filling and increased vessel pruning (Figure 4A and B).

Next, we subjected mice to the adTGFβ-induced pulmonary fibrosis and the lung tissues were analysed for vascular rarefaction. Expression with adTGFβ leads to significant pruning of small vessels on day 8 compared with adControl (Figure 4C and D). TCBN treatment maintained the vasculature even in the presence of adTGFβ whereas rapamycin-
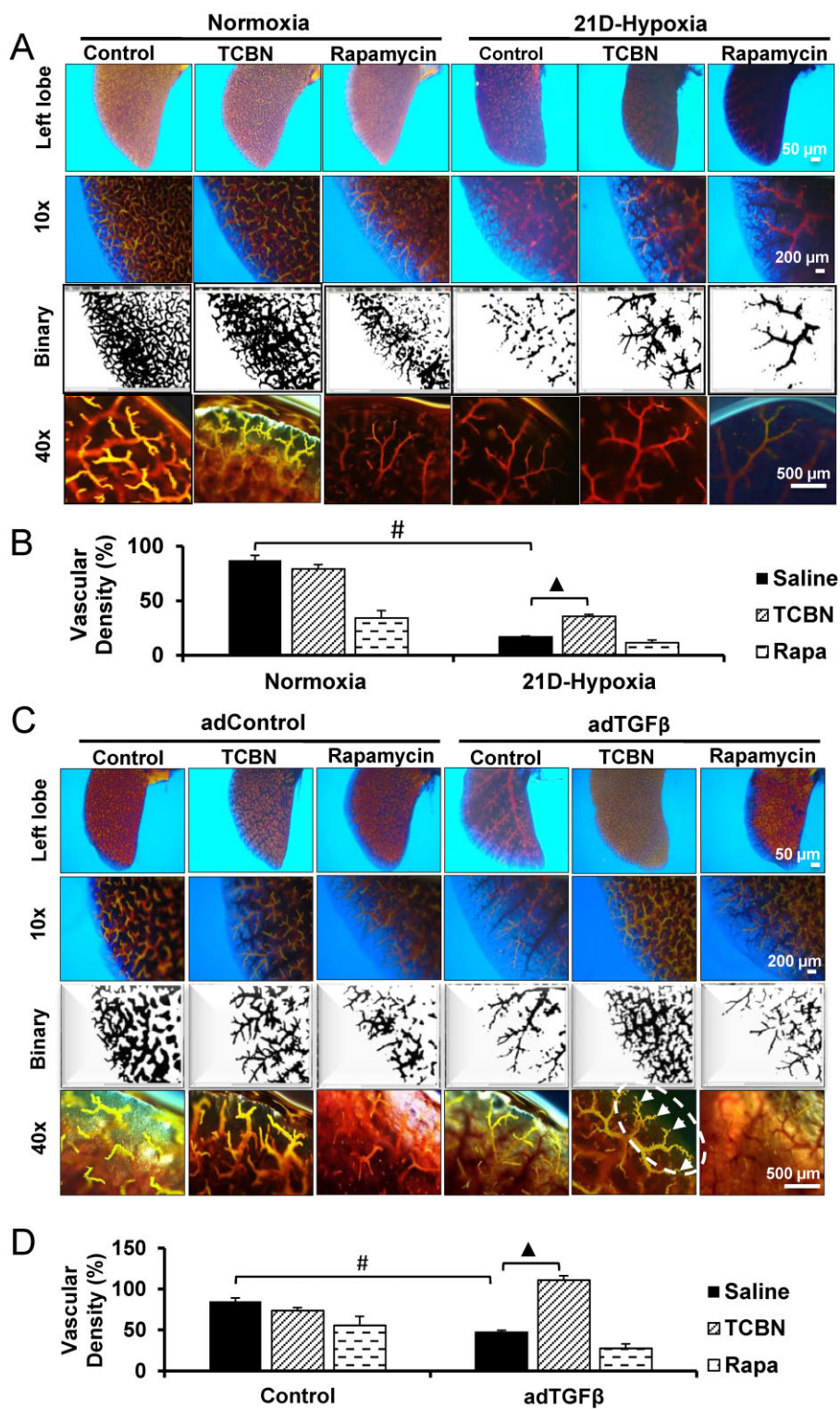
Figure 4

TCBN reverses hypoxia- and adTGFβ-induced vascular rarefaction. (A) Representative images showing vascular branching of the left lobe after Microfil casting of mice subjected to normoxia or chronic hypoxia and treated with saline, TCBN or rapamycin. (B) Histogram showing vascular density (%) in mouse lungs subjected to normoxia or chronic hypoxia and treated with saline, TCBN or rapamycin, and calculated using ImageJ software ($n = 3$–5 mice/group). (C) Representative images showing vascular branching of the left lobe after Microfil casting of mice subjected to adControl or adTGFβ, and treated with saline, TCBN or rapamycin. Arrows indicate increase in microvascular branching in TCBN-treated group. (D) Histogram showing vascular density (%) in mouse lungs subjected to adControl or adTGFβ treated with saline, TCBN or rapamycin, and calculated using ImageJ software ($n = 3$–5 mice/group). [#]$P < 0.01$, ▲$P < 0.001$. Scale bar in order 500, 200 and 50 μm.

treated mice did not show a beneficial effect on peripheral vasculature protection (Figure 4C and D).

Akt inhibition ameliorates chronic hypoxia-induced right ventricular remodelling and hepatotoxicity

The hypoxia-induced pulmonary vasculopathies often lead to right ventricular hypertrophy (Voelkel *et al.*, 2012). We determined the effects of inhibiting Akt or mTOR on right ventricular wall thickness in mice subjected to 21 day hypoxia. Under normoxic conditions, neither TCBN nor rapamycin induced any discernible effects on wall thickness (Figure 5A and B). The modest but significant increase in right ventricular wall thickness in hypoxic compared with normoxic mice was reversed by TCBN treatment (Figure 5A and B). However, rapamycin treatment did not induce a significant reduction in right ventricular wall thickness (Figure 5A and B).

Next, we assessed the safety profile of both drugs in the liver of mice subjected to chronic hypoxia. Compared with normoxia control, liver sections from 21 day chronic hypoxic mice exhibited significantly higher percentage of gap areas between the cells indicating significant liver damage due to hypoxia (Figure 5C and D). This is evident from the marked degeneration and atrophy of hepatic cords and the associated sinusoidal dilation. Liver histology also revealed that treatment with TCBN, but not rapamycin, blunted liver damage due to chronic hypoxia (Figure 5C and D). No significant difference in the ratio between lung, liver, heart or kidney weights and total body weight was observed, thus suggesting that both TCBN and rapamycin had no severe toxic effects on mice (Supporting Information Fig. S1).

Akt1 inhibition attenuates pulmonary remodelling through inhibition of TSP1 expression

To identify the signalling molecules downstream of Akt1 activation in pulmonary fibrosis, we performed gene arrays for fibrosis-related genes in both NIH-3T3 and FHLFs expressing inactive mutant of Akt1 (DN-Akt1; Akt1 K179M). A common target identified from gene arrays performed in both the cells after Akt1 inhibition was reduced expression of TSP1 (Figure 6A). Indeed, Western analyses revealed that the TSP1 expression in 14d-hypoxic $Akt1^{+/+}$ mice was blunted in 14d-hypoxic $Akt1^{-/-}$ mice, which was also correlated with significantly reduced fibronectin expression (Figure 6B and C).

To further confirm our previous *in vivo* and *in vitro* findings, we subjected FHLFs isolated from an IPF patient to serum starvation and treated with 10 nM TCBN or 25 nM rapamycin for 24 h, and analysed αSMA, fibronectin and TSP1 expression levels. Inhibiting Akt, but not mTOR, significantly reduced αSMA, fibronectin and TSP1 expressions in FHLFs (Figure 6D and E). The results were confirmed *in vivo* using Western analysis of the adControl and adTGFβ expressing mice lung tissues. Our analysis indicated that the lungs expressing adTGFβ expressed significantly higher concentrations of TSP1 along with the expression of increased expression of myofibroblast markers such as αSMA, ED-A-FN and ECM proteins, and that treatment with TCBN, but not rapamycin, significantly reversed their expression (Figure 7A and B).

TSP1$^{-/-}$ mice are protected from adMyrAkt1-induced pulmonary fibrosis

To further confirm the causal role of Akt1-TSP1 signalling axis in PF and lung tissue remodelling, we subjected $TSP1^{+/+}$ and $TSP1^{-/-}$ mice to i.t. administration of adenovirus-mediated gene transfer of control vector or adenovirus-mediated expression of constitutively active Akt1 (adMyrAkt1). Administration of adMyrAkt1 in mice resulted in significant interstitial fibrosis. $TSP1^{+/+}$ lung tissues expressing adMyrAkt1 exhibited significant increase in tissue remodelling correlating an Aschroft scale of ~7 (Figure 8A–C). Although mild tissue remodelling was already present in $TSP1^{-/-}$ mice lungs, compared with control-$TSP1^{+/+}$ mice, $TSP1^{-/-}$ mice did not exhibit significant histological alterations with adMyrAkt1 expression (Figure 8A–C), thus indicating that $TSP1^{-/-}$ mice are resistant to adMyrAkt1-induced pulmonary fibrosis (Figure 7A–C).

Discussion and conclusions

Although Akt is hyperactivated in the fibroblastic foci in human IPF lungs (Xia *et al.*, 2008), a causal link between Akt activation and the events leading to IPF has not been established. Further, the therapeutic benefits of targeting Akt for IPF have not yet been investigated. Our major findings from the current study are: (i) $Akt1^{-/-}$ mice are protected from chronic hypoxia-induced pulmonary vascular and tissue remodelling; (ii) Akt inhibitor TCBN ameliorates progressive chronic hypoxia- and adTGFβ-induced pulmonary fibrosis, peripheral vascular remodelling and rarefaction; (iii) targeting Akt substrate mTOR using rapamycin did not reverse chronic hypoxia- and adTGFβ-induced peripheral vascular remodelling and rarefaction, and pulmonary fibrosis, respectively; (iv) genetic ablation of Akt1 and pharmacological inhibition of Akt both resulted in significantly reduced expression of TSP1, a matricellular protein known to be involved in the hypoxia-induced pulmonary remodelling (Ochoa *et al.*, 2010) as well as fibrosis progression (Bussolati *et al.*, 2006; Xie *et al.*, 2010); (v) sustained hyperactivation of Akt1 in the mice lungs through expression of adMyrAkt1-induced severe pulmonary fibrosis even in the absence of any TGFβ stimuli; and (vi) $TSP1^{-/-}$ mice are protected from adMyrAkt1-induced pulmonary fibrosis. Our study demonstrates the integral role of Akt1 in the disease progression of IPF through development of fibrotic foci and vascular rarefaction, partly through modulation of TSP1, ED-A-FN and collagen type I expression, in addition to its role in the expression of αSMA via a SRF/myocardin pathway. To our knowledge, these findings are novel and have not been reported previously.

The origin of the events leading to the development of IPF is still not clearly understood. This also became the bottleneck in the development of the appropriate treatment strategy for pulmonary fibrosis patients. A variety of theories such as 'vascular', 'plasticity/growth factor receptor', 'inflammation' and 'matrix' hypotheses have been proposed for the development of IPF (Bringardner *et al.*, 2008). Others have argued that profound inflammation in the alveoli and the interstitium is the major cause of IPF (Gauldie, 2002; Strieter, 2002). However, clinical trials on anti-inflammatory agents
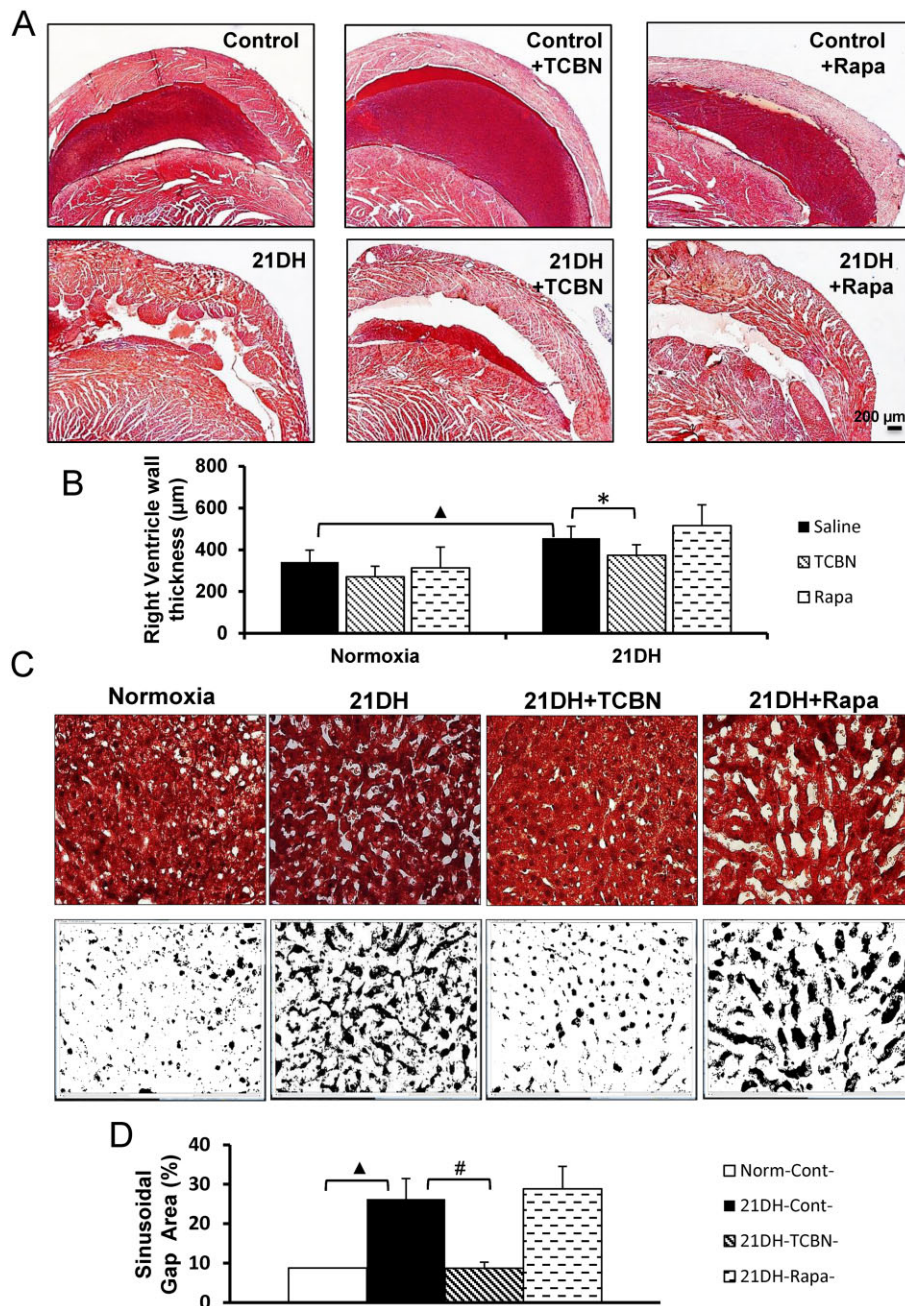
Figure 5

TCBN inhibits hypoxia-induced right ventricular remodelling and hepatic injury. (A) Images of Masson's trichrome stained cross sections of the right ventricle from control, chronic hypoxic, hypoxic treated with TCBN and hypoxic treated with rapamycin hearts. (B) Histogram showing quantification of right ventricular wall thickness showing the effect of TCBN and rapamycin on compensatory ventricular wall remodelling following hypoxia ($n = 6$–8 mice/group). (C) Pictures of Masson's trichrome stained liver sections and binary images (using ImageJ software). (D) Histogram showing quantification of per cent sinusoidal gap area as measured using ImageJ software from binary images ($n = 6$–8 mice/group). $*P < 0.05$, $^{#}P < 0.01$, $^{\blacktriangle}P < 0.001$.

for the treatment of IPF patients did not yield beneficial effects (Rafii *et al.*, 2013). Even though thrombin and tissue factor expression was enhanced in IPF lungs suggesting a role for platelets in the disease progression, heparin or warfarin provided no therapeutic benefits (Kubo *et al.*, 2005). Although vascular remodelling occurs in fibrosis (Barman

et al., 2014), the VEGF inhibitor SU5416 (SUGEN) induces pulmonary vascular injury and remodelling leading to PH (Mendel *et al.*, 2000). Although PH has been linked to the development of ILD, its management has proven ineffective in IPF patients. Clinical trials of the endothelin receptor antagonist bosentan used in the management of PH failed
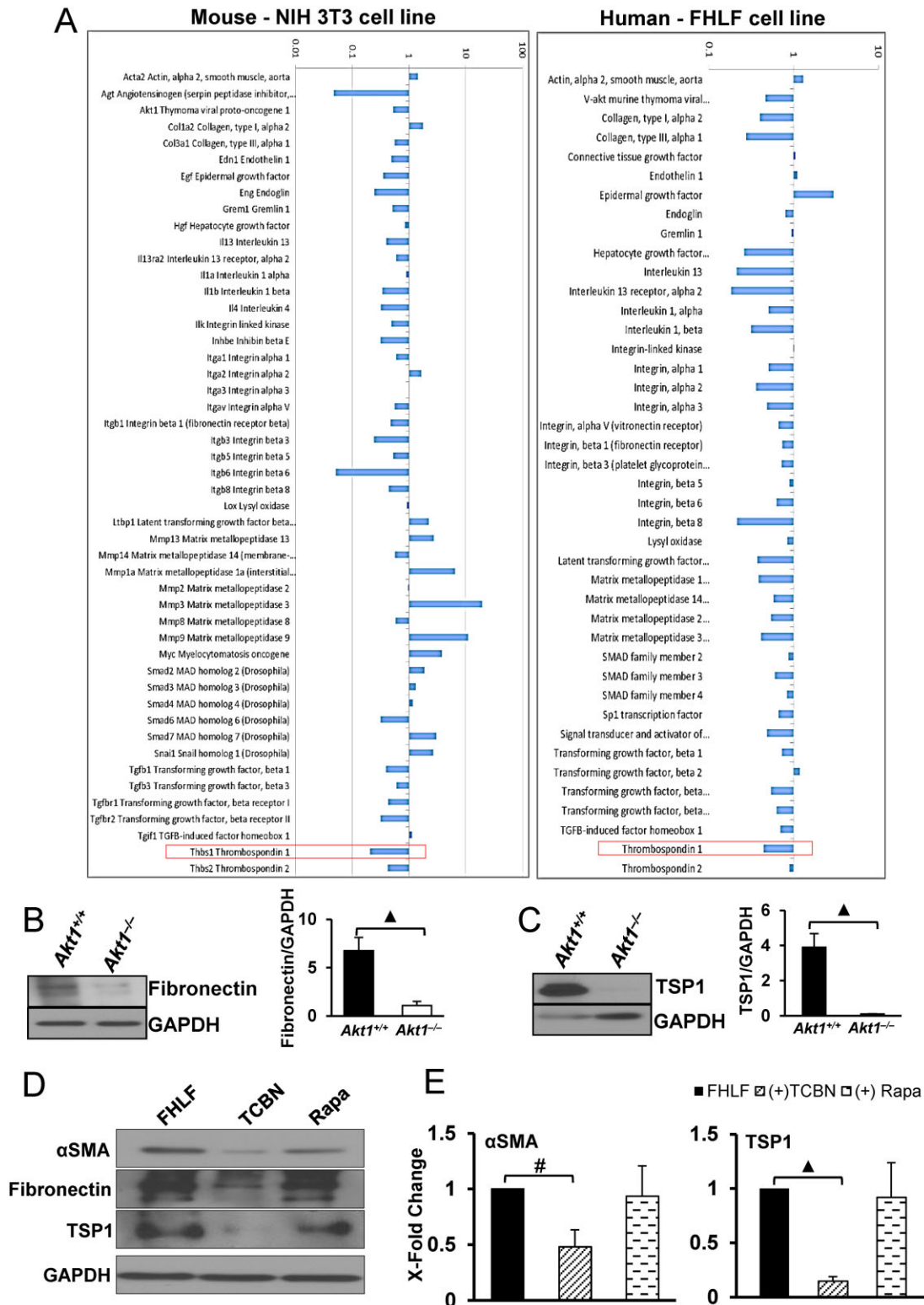
Figure 6

TSP1 expression is decreased in Akt1-deficient NIH 3T3, IPF fibroblasts and 14 day hypoxic mice. (A) Gene expression profiles of NIH 3T3 and IPF fibroblasts (FHLFs) expressing DN-Akt1 (dominant negative, inactive Akt1) ($n = 3$). (B and C) Western blot image and histogram showing total fibronectin and TSP1 expression levels normalized to GAPDH levels in 14 day hypoxic $Akt1^{+/+}$ and $Akt1^{-/-}$ mice lungs ($n = 3$–5 per group). (D) Images of Western blots showing the effect of TCBN and rapamycin on the expression of αSMA and TSP1 expression in FHLFs. (E) Histogram showing densitometry analysis of the Western blot bands indicating changes in the expression levels of αSMA and TSP1, normalized to GAPDH after treatment with TCBN and rapamycin in FHLFs ($n = 3$). $^{#}P < 0.01$, $^{▲}P < 0.001$.
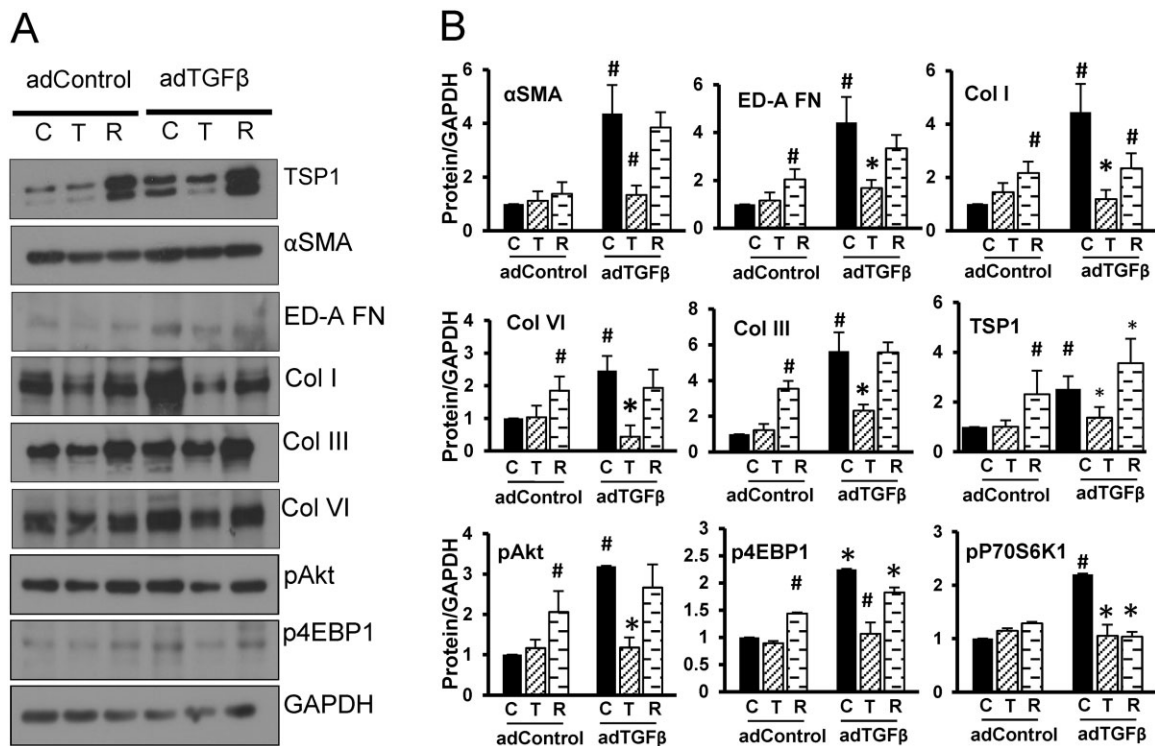
Figure 7

Targeting Akt, not mTOR, modulates expression of TSP1, αSMA and ECM proteins in the mice lungs with adTGFβ expression. (A) Western blot images of adControl and adTGFβ expressing lung tissue lysates showing the changes in expression of TSP1, αSMA, ED-A-FN, collagens (types I, III and VI), and phosphorylated Akt and 4E-BP1. (B) Densitometry analysis of Western blot bands of adControl and adTGFβ-expressing lung tissue lysates showing the changes in expression of TSP1, αSMA, ED-A-FN, collagens (types I, III and VI) and phosphorylated Akt and 4E-BP1 ($n = 4$). *$P < 0.05$, #$P < 0.01$.

clinical trials in IPF patients (Rafii *et al.*, 2013). In contrast, nintedanib, a broad spectrum receptor tyrosine kinase inhibitor, improved the quality of life for IPF patients (Richeldi *et al.*, 2014). On the other hand, the pathological hallmark of fibrosis is the persistent myofibroblast differentiation and ECM deposition. TGFβ is the major mediator of tissue fibrosis through promotion of myofibroblast differentiation and ECM deposition (Tomasek *et al.*, 2002; Hinz *et al.*, 2012). A recent clinical trial on pirfenidone, an inhibitor of TGFβ, demonstrated very similar efficacy to that of nintedanib in IPF patients (Takeda *et al.*, 2014). Although these two studies demonstrated improvement in the forced vital capacity in IPF patients leading to its approval for use in the USA by the Food and Drug Administration in 2014, unfortunately neither of these had any significant effect on the overall patient mortality. These clinical trials provided important clues that a multifactorial disease such as IPF cannot be treated by targeting just one arm of the disease.

Intracellular signalling molecules such as the PI3 kinase-Akt pathway, Ras-mitogen activated kinase (MAPK) pathway and Rho-GTPase signalling are activated by various receptor tyrosine kinases, GPCRs and TGFβ family of growth factors (Massagué, 2012). Among these, Akt is a potential target for IPF therapy due to its involvement in various processes leading to the development of IPF. We have previously demonstrated that Akt1, the predominant Akt isoform in

endothelial cells and fibroblasts, is responsible for the promotion of angiogenesis and vascular protection (Chen *et al.*, 2005a), wound healing (Somanath *et al.*, 2008), and fibroblast-mediated ECM secretion (Goc *et al.*, 2011) and assembly (Somanath *et al.*, 2007; Somanath and Byzova, 2009). Akt1 has also been implicated in the regulation of pulmonary artery neointimal proliferation through smooth muscle cell activation (Tang *et al.*, 2015). In pathological conditions, Akt1 also promoted myofibroblast differentiation *in vitro* (Abdalla *et al.*, 2013) and post-ischaemic cardiac fibrosis *in vivo* (Ma *et al.*, 2014). Furthermore, whereas Akt1 inhibition has been shown to induce vascular permeability, specific role for each of the Akt1, Akt2 and Akt3 isoforms has been implicated in platelet activation and thrombosis (Chen *et al.*, 2004; Woulfe *et al.*, 2004; O'Brien *et al.*, 2011). Akt1 has also been shown to promote inflammation (Di Lorenzo *et al.*, 2009). Several lines of evidence have reported that PI3K/Akt pathway is hyperactivated during fibrosis in general (Xia *et al.*, 2010) and pulmonary fibrosis in particular (Xia *et al.*, 2008). As events leading to the vascular complications and pulmonary tissue remodelling are consistent with deregulated Akt-mediated cellular and molecular processes, we hypothesized that hyperactivation of Akt would lead to pathological pulmonary tissue remodelling, and that pharmacological inhibition of Akt might be a logical solution for the treatment of IPF patients. Our data from *Akt1*$^{-/-}$ mice
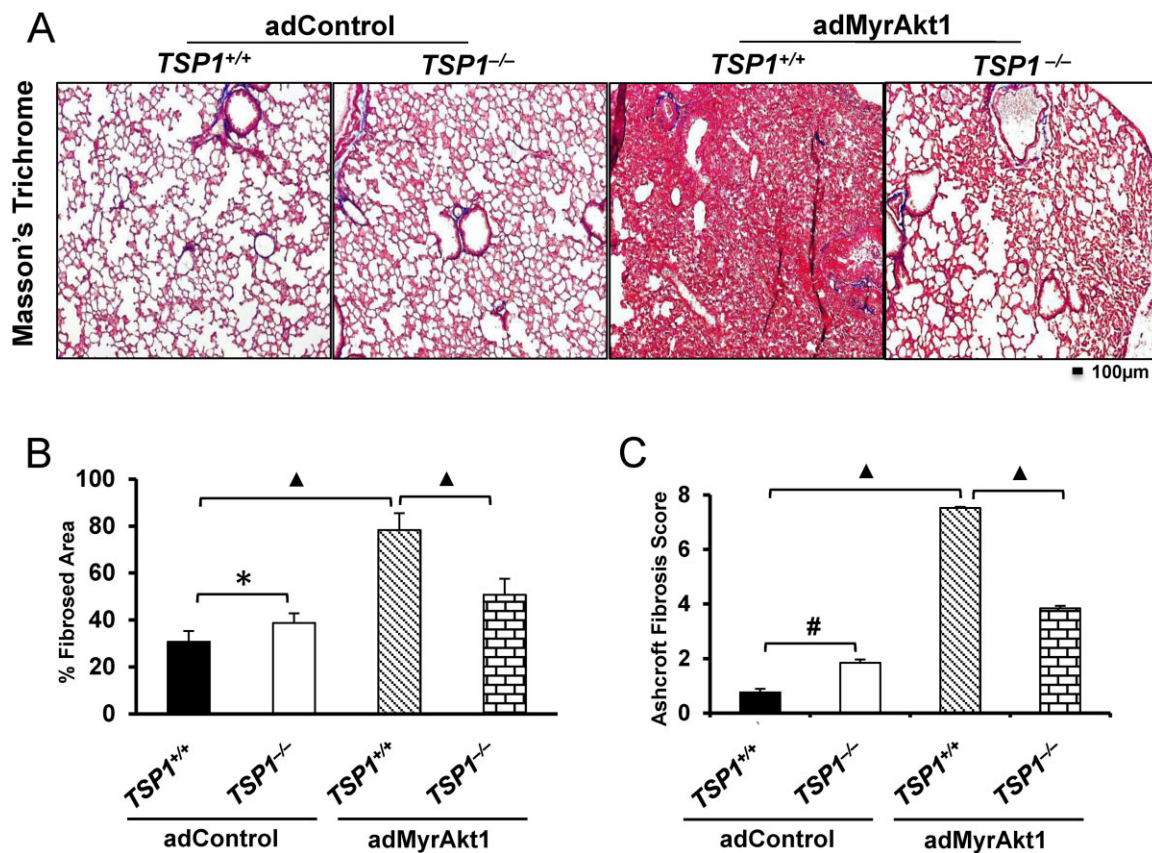
Figure 8

TSP1⁻/⁻ mice are protected from adMyrAkt1-induced pulmonary fibrosis. (A) Masson's trichrome staining of *WT* and *TSP1⁻/⁻* mouse lung harvested 14 days after i.t. adenovirus gene transfer of control vector or adMyrAkt1 (constitutive active Akt1) ($n = 3$ mice/group). (B and C) Per cent fibrosed area quantified using ImageJ software, and Ashcroft fibrosis score of the degree of fibrosis in *WT* and *TSP1⁻/⁻* mice subjected to control vector or adMyr-Akt1 respectively. *$P < 0.05$, #$P < 0.01$, ▲$P < 0.001$.

lungs showing impaired chronic hypoxia-induced pulmonary tissue and vascular remodelling evidenced by reduced interstitial lesions associated with decreased expression of fibronectin and αSMA further supported this hypothesis.

Currently, TCBN, an Akt inhibitor, is in clinical trials for the management of various types of cancers, and initial reports indicate no serious adverse events (Garrett *et al.*, 2011). Its specificity and efficacy in cancer prompted us to test this drug in comparison with the anti-inflammatory mTOR inhibitor rapamycin. Our study identified anti-fibrotic and anti-remodelling properties of TCBN as evident by the reduced fibrotic lesions, αSMA and matrix deposition, decreased medial thickening of pulmonary arterioles, reduced vascular pruning and right ventricular thickening. In contrast, rapamycin exacerbated the conditions through increased alveolar congestion and micro-haemorrhage, severe pulmonary vascular rarefaction, right ventricular thickening and hepatotoxicity. Rapamycin did not induce anti-fibrotic and anti-remodelling response as previously reported in rodent models (Paddenberg *et al.*, 2007; Korfhagen *et al.*, 2009). Whereas one potential reason for this discrepancy could be due to the use of supra-optimal doses of rapamycin (4 and 3 mg·kg⁻¹·day⁻¹ respectively) in these studies, our results are consistent with clinical reports of pulmonary tox-

icities associated with two rapamycin derivatives, sirolimus and everolimus (Buhaescu *et al.*, 2006; Damas *et al.*, 2006; Khalife *et al.*, 2007; Feagans *et al.*, 2009; Depuydt *et al.*, 2012). Importantly, this finding sheds light on the adverse effects of everolimus observed in IPF patients (Malouf *et al.*, 2011). Mechanistically, the adverse effects of rapamycin could be attributed, at least in part, to the rebound Akt activation as reported by several laboratories (Sun *et al.*, 2005; Breuleux *et al.*, 2009; Zakikhani *et al.*, 2010; Soares *et al.*, 2013). On the other hand, TCBN exhibits dual role by targeting both myofibroblast differentiation and the ECM deposition, in addition to increasing vascular perfusion, platelet inactivation and reduced inflammation as reported in the literature. This suggests that targeting Akt, not mTOR, may serve as a favourable therapeutic strategy in IPF.

Our previous study has identified that Akt1 is directly involved in TSP1 expression by the vascular cells, and *Akt1⁻/⁻* mice skin and lung endothelial cells express reduced levels of TSP1 (Chen *et al.*, 2005b). Interestingly, it has been shown that TSP1 deficiency protects against hypoxia-induced PH (Ochoa *et al.*, 2010), but not in bleomycin-induced pulmonary fibrosis (Ezzie *et al.*, 2012). Increased TSP1 has also been shown to promote vascular rarefaction (Gonzalez-Quesada *et al.*, 2013). Incidentally, our gene array analysis in two

different fibroblast cell lines, murine NIH 3T3 and human pulmonary fibrosis patient lung fibroblasts, also identified decreased TSP1 gene expression upon overexpression with DN-Akt1 (Akt1K179M inactive mutant). This was further confirmed at the protein level in $Akt1^{-/-}$ mice lungs and human fibrotic lung fibroblasts. As overexpression with adMyrAkt1 in lungs was sufficient to cause fibrosis, and because bleomycin was able to induce fibrosis $TSP1^{-/-}$ mice lungs, we determined whether $TSP1^{-/-}$ mice lungs will be resistant to pulmonary fibrosis induced by adMyrAkt1 overexpression. We found that TSP1-deficient mice are protected from adMyrAkt1-induced pulmonary fibrosis. The reason that $TSP1^{-/-}$ mice lungs were resistant to bleomycin-induced pulmonary fibrosis, but not to adMyrAkt1-induced pulmonary vascular remodelling along with our observation of pulmonary tissue remodelling in $Akt1^{-/-}$ mice lungs in normoxic conditions, suggests the existence of Akt-independent pathways in the regulation of TGFβ-induced pulmonary fibrosis. Collectively, our results provide direct evidence on the causal role of Akt1 in disease onset and progression in pulmonary fibrosis by promoting myofibroblast differentiation and ECM deposition, in part, through TSP1 regulation. Our study indicates potential therapeutic benefits of the Akt inhibitor TCBN for the treatment of ILD, particularly IPF.

Acknowledgements

Author contributions

M. A., H. S. and R. P. performed the research. M. A., A. E., S. C. F. and P. R. S. designed the research study. M. A., H. S., R. P. and P. R. S. analysed the data. M. A. and P. R. S. wrote the paper.

Conflict of interest

The authors have declared that no conflicts of interest exist.

References

Abdalla M, Goc A, Segar L, Somanath PR (2013). Akt1 mediates α-smooth muscle actin expression and myofibroblast differentiation via myocardin and serum response factor. J Biol Chem 288: 33483–33493.

Alexander SPH, Benson HE, Faccenda E, Pawson AJ, Sharman JL, Spedding M et al.; CGTP Collaborators (2013). The Concise Guide to PHARMACOLOGY 2013/14: Enzymes. Br J Pharmacol 170: 1797–1867.

Ashcroft T, Simpson JM, Timbrell V (1988). Simple method of estimating severity of pulmonary fibrosis on a numerical scale. J Clin Pathol 41: 467–470.

Barman SA, Chen F, Su Y, Dimitropoulou C, Wang Y, Catravas JD et al. (2014). Nadph oxidase 4 is expressed in pulmonary artery adventitia and contributes to hypertensive vascular remodeling. Arterioscler Thromb Vasc Biol 34: 1704–1715.

Breuleux M, Klopfenstein M, Stephan C, Doughty CA, Barys L, Maira SM et al. (2009). Increased AKT S473 phosphorylation after mTORC1 inhibition is rictor dependent and does not predict tumor cell response to PI3K/mTOR inhibition. Mol Cancer Ther 8: 742–753.

Bringardner BD, Baran CP, Eubank TD, Marsh CB (2008). The role of inflammation in the pathogenesis of idiopathic pulmonary fibrosis. Antioxid Redox Signal 10: 287–301.

Buhaescu I, Izzedine H, Covic A (2006). Sirolimus-challenging current perspectives. Ther Drug Monit 28: 577–584.

Bussolati B, Assenzio B, Deregibus MC, Camussi G (2006). The proangiogenic phenotype of human tumor-derived endothelial cells depends on thrombospondin-1 downregulation via phosphatidylinositol 3-kinase/Akt pathway. J Mol Med (Berl) 84: 852–863.

Chen J, De S, Damron DS, Chen WS, Hay N, Byzova TV (2004). Impaired platelet responses to thrombin and collagen in AKT-1-deficient mice. Blood 104: 1703–1710.

Chen J, Somanath PR, Razorenova O, Chen WS, Hay N, Bornstein P et al. (2005a). Akt1 regulates pathological angiogenesis, vascular maturation and permeability in vivo. Nat Med 11: 1188–1196.

Chen YL, Law PY, Loh HH (2005b). Inhibition of PI3K/Akt signaling: an emerging paradigm for targeted cancer therapy. Curr Med Chem Anticancer Agents 5: 575–589.

Damas C, Oliveira A, Morais A (2006). Lung toxicity induced by rapamycin. Rev Port Pneumol 12: 715–724.

Depuydt P, Nollet J, Benoit D, Praet M, Caes F (2012). Fatal acute pulmonary injury associated with everolimus. Ann Pharmacother 46: e7.

Di Lorenzo A, Fernández-Hernando C, Cirino G, Sessa WC (2009). Akt1 is critical for acute inflammation and histamine-mediated vascular leakage. Proc Natl Acad Sci U S A 106: 14552–14557.

Ezzie ME, Crawford M, Cho JH, Orellana R, Zhang S, Gelinas R et al. (2012). Gene expression networks in COPD: microRNA and mRNA regulation. Thorax 67: 122–131.

Feagans J, Victor D, Moehlen M, Florman SS, Regenstein F, Balart LA et al. (2009). Interstitial pneumonitis in the transplant patient: consider sirolimus-associated pulmonary toxicity. J la State Med Soc 161: 166, 168–172.

Garrett CR, Coppola D, Wenham RM, Cubitt CL, Neuger AM, Frost TJ et al. (2011). Phase I pharmacokinetic and pharmacodynamic study of triciribine phosphate monohydrate, a small-molecule inhibitor of AKT phosphorylation, in adult subjects with solid tumors containing activated AKT. Invest New Drugs 29: 1381–1389.

Gauldie J (2002). Pro: inflammatory mechanisms are a minor component of the pathogenesis of idiopathic pulmonary fibrosis. Am J Respir Crit Care Med 165: 1205–1206.

Goc A, Choudhary M, Byzova TV, Somanath PR (2011). TGFβ- and bleomycin-induced extracellular matrix synthesis is mediated through Akt and mammalian target of rapamycin (mTOR). J Cell Physiol 226: 3004–3013.

Gonzalez-Quesada C, Cavalera M, Biernacka A, Kong P, Lee DW, Saxena A et al. (2013). Thrombospondin-1 induction in the diabetic myocardium stabilizes the cardiac matrix in addition to promoting vascular rarefaction through angiopoietin-2 upregulation. Circ Res 113: 1331–1344.

Hinz B, Phan SH, Thannickal VJ, Prunotto M, Desmoulière A, Varga J et al. (2012). Recent developments in myofibroblast biology: paradigms for connective tissue remodeling. Am J Pathol 180: 1340–1355.

Khalife WI, Kogoj P, Kar B (2007). Sirolimus-induced alveolar hemorrhage. J Heart Lung Transplant 26: 652–657.

Kilkenny C, Browne W, Cuthill IC, Emerson M, Altman DG (2010). Animal research: Reporting in vivo experiments: the ARRIVE guidelines. Br J Pharmacol 160: 1577–1579.

King TE, Pardo A, Selman M (2011). Idiopathic pulmonary fibrosis. Lancet 378: 1949–1961.

Korfhagen TR, Le Cras TD, Davidson CR, Schmidt SM, Ikegami M, Whitsett JA et al. (2009). Rapamycin prevents transforming growth factor-alpha-induced pulmonary fibrosis. Am J Respir Cell Mol Biol 41: 562–572.

Kubo H, Nakayama K, Yanai M, Suzuki T, Yamaya M, Watanabe M et al. (2005). Anticoagulant therapy for idiopathic pulmonary fibrosis. Chest 128: 1475–1482.

Ma L, Kerr BA, Naga Prasad SV, Byzova TV, Somanath PR (2014). Differential effects of Akt1 signaling on short- versus long-term consequences of myocardial infarction and reperfusion injury. Lab Invest 94: 1083–1091.

Malouf MA, Hopkins P, Snell G, Glanville AR, Investigators EiIS (2011). An investigator-driven study of everolimus in surgical lung biopsy confirmed idiopathic pulmonary fibrosis. Respirology 16: 776–783.

Massagué J (2012). TGFβ signalling in context. Nat Rev Mol Cell Biol 13: 616–630.

McGrath J, Drummond G, McLachlan E, Kilkenny C, Wainwright C (2010). Guidelines for reporting experiments involving animals: the ARRIVE guidelines. Br J Pharmacol 160: 1573–1576.

McLaughlin VV, Archer SL, Badesch DB, Barst RJ, Farber HW, Lindner JR et al. (2009). ACCF/AHA 2009 expert consensus document on pulmonary hypertension a report of the American College of Cardiology Foundation Task Force on Expert Consensus Documents and the American Heart Association developed in collaboration with the American College of Chest Physicians; American Thoracic Society, Inc.; and the Pulmonary Hypertension Association. J Am Coll Cardiol 53: 1573–1619.

Mendel DB, Schreck RE, West DC, Li G, Strawn LM, Tanciongco SS et al. (2000). The angiogenesis inhibitor SU5416 has long-lasting effects on vascular endothelial growth factor receptor phosphorylation and function. Clin Cancer Res 6: 4848–4858.

Meyer KC (2014). Diagnosis and management of interstitial lung disease. Transl Respir Med 2: 4.

O'Brien KA, Stojanovic-Terpo A, Hay N, Du X (2011). An important role for Akt3 in platelet activation and thrombosis. Blood 118: 4215–4223.

Ochoa CD, Yu L, Al-Ansari E, Hales CA, Quinn DA (2010). Thrombospondin-1 null mice are resistant to hypoxia-induced pulmonary hypertension. J Cardiothorac Surg 5: 32.

Paddenberg R, Stieger P, von Lilien AL, Faulhammer P, Goldenberg A, Tillmanns HH et al. (2007). Rapamycin attenuates hypoxia-induced pulmonary vascular remodeling and right ventricular hypertrophy in mice. Respir Res 8: 15.

Pawson AJ, Sharman JL, Benson HE, Faccenda E, Alexander SP, Buneman OP et al.; NC-IUPHAR (2014). The IUPHAR/BPS Guide to PHARMACOLOGY: an expert-driven knowledge base of drug targets and their ligands. Nucl Acids Res 42 (Database Issue): D1098–D1106.

Rafii R, Juarez MM, Albertson TE, Chan AL (2013). A review of current and novel therapies for idiopathic pulmonary fibrosis. J Thorac Dis 5: 48–73.

Raghu G, Collard HR, Egan JJ, Martinez FJ, Behr J, Brown KK et al. (2011). An official ATS/ERS/JRS/ALAT statement: idiopathic pulmonary fibrosis: evidence-based guidelines for diagnosis and management. Am J Respir Crit Care Med 183: 788–824.

Richeldi L, du Bois RM, Raghu G, Azuma A, Brown KK, Costabel U et al. (2014). Efficacy and safety of nintedanib in idiopathic pulmonary fibrosis. N Engl J Med 370: 2071–2082.

Soares HP, Ni Y, Kisfalvi K, Sinnett-Smith J, Rozengurt E (2013). Different patterns of Akt and ERK feedback activation in response to rapamycin, active-site mTOR inhibitors and metformin in pancreatic cancer cells. PLoS ONE 8: e57289.

Somanath PR, Byzova TV (2009). 14-3-3beta-Rac1-p21 activated kinase signaling regulates Akt1-mediated cytoskeletal organization, lamellipodia formation and fibronectin matrix assembly. J Cell Physiol 218: 394–404.

Somanath PR, Kandel ES, Hay N, Byzova TV (2007). Akt1 signaling regulates integrin activation, matrix recognition, and fibronectin assembly. J Biol Chem 282: 22964–22976.

Somanath PR, Chen J, Byzova TV (2008). Akt1 is necessary for the vascular maturation and angiogenesis during cutaneous wound healing. Angiogenesis 11: 277–288.

Strange C, Highland KB (2005). Pulmonary hypertension in interstitial lung disease. Curr Opin Pulm Med 11: 452–455.

Strieter RM (2002). Con: inflammatory mechanisms are not a minor component of the pathogenesis of idiopathic pulmonary fibrosis. Am J Respir Crit Care Med 165: 1206–1207, discussion 1207–1208.

Sun SY, Rosenberg LM, Wang X, Zhou Z, Yue P, Fu H et al. (2005). Activation of Akt and eIF4E survival pathways by rapamycin-mediated mammalian target of rapamycin inhibition. Cancer Res 65: 7052–7058.

Takeda Y, Tsujino K, Kijima T, Kumanogoh A (2014). Efficacy and safety of pirfenidone for idiopathic pulmonary fibrosis. Patient Prefer Adherence 8: 361–370.

Tang H, Chen J, Fraidenburg DR, Song S, Sysol JR, Drennan AR et al. (2015). Deficiency of Akt1, but Not Akt2, attenuates the development of pulmonary hypertension. Am J Physiol Lung Cell Mol Physiol 308: L208–L220.

Tomasek JJ, Gabbiani G, Hinz B, Chaponnier C, Brown RA (2002). Myofibroblasts and mechano-regulation of connective tissue remodelling. Nat Rev Mol Cell Biol 3: 349–363.

Voelkel NF, Gomez-Arroyo J, Abbate A, Bogaard HJ, Nicolls MR (2012). Pathobiology of pulmonary arterial hypertension and right ventricular failure. Eur Respir J 40: 1555–1565.

Woulfe D, Jiang H, Morgans A, Monks R, Birnbaum M, Brass LF (2004). Defects in secretion, aggregation, and thrombus formation in platelets from mice lacking Akt2. J Clin Invest 113: 441–450.

Xia H, Diebold D, Nho R, Perlman D, Kleidon J, Kahm J *et al.* (2008). Pathological integrin signaling enhances proliferation of primary lung fibroblasts from patients with idiopathic pulmonary fibrosis. J Exp Med 205: 1659–1672.

Xia H, Khalil W, Kahm J, Jessurun J, Kleidon J, Henke CA (2010). Pathologic caveolin-1 regulation of PTEN in idiopathic pulmonary fibrosis. Am J Pathol 176: 2626–2637.

Xie XS, Liu HC, Wang FP, Zhang CL, Zuo C, Deng Y *et al.* (2010). Ginsenoside Rg1 modulation on thrombospondin-1 and vascular endothelial growth factor expression in early renal fibrogenesis in unilateral obstruction. Phytother Res 24: 1581–1587.

Zakikhani M, Blouin MJ, Piura E, Pollak MN (2010). Metformin and rapamycin have distinct effects on the AKT pathway and proliferation in breast cancer cells. Breast Cancer Res Treat 123: 271–279.

Supporting information

Additional Supporting Information may be found in the online version of this article at the publisher's web-site:

http://dx.doi.org/10.1111/bph.13203

Figure S1 Effect of triciribine and rapamycin on organ and body weight during hypoxia. The ratio of organ to body weight was quantified for the lung, heart, liver and kidney ($n = 6$–8 mice/group).